Journal of Inorganic and General Chemistry
ZAAC
Zeitschrift für anorganische und allgemeine Chemie
DOI: 10.1002/zaac.201900189
ARTICLE

Single Crystals of $CaNa[ReO_4]_3$: Serendipitous Formation and Systematic Characterization

Maurice Conrad[a] and Thomas Schleid*[a]

Dedicated to Professor Martin Jansen on the Occasion of his 75th Birthday

Abstract. In an attempt to crystallize $Ce[ReO_4]_4 \cdot xH_2O$ from aqueous solutions of equimolar amounts of $Ce[SO_4]_2$ and $Ba[ReO_4]_2$ via salt-metathesis the serendipitous formation of colorless, transparent, rod-shaped single crystals of $CaNa[ReO_4]_3$ was observed as a result of calcium and sodium impurities within the improperly deionized water used. Structure analysis by X-ray diffraction lead to the conclusion that the title compound crystallizes in the $ThCd[MoO_4]_3$ structure type with the hexagonal space group $P6_3/m$ and the lattice parameters a = 991.74(6) pm, c = 636.53(4) pm, c/a = 0.642 for Z = 2. The crystal structure contains purely oxygen surrounded and crystallographically unique cations, namely Ca^{2+} in tricapped trigonal prismatic (d(Ca–O) = 6 × 249 pm + 3 × 254 pm), Na^+ in octahedral (d(Na–O) = 6 × 241 pm), and Re^{7+} in tetrahedral coordination (d(Re–O) = 171–173 pm). Furthermore, it was possible to yield an almost phase-pure microcrystalline powder of the title compound from a melt of equimolar amounts of $Na[ReO_4]$ and $Ca[ReO_4]_2$ stemming from aquatically obtained precursors.

Introduction

The scientific oeuvre of *Martin Jansen* has a strong pronunciation on solid-state oxides, which covers binary alkali-metal oxides with strange oxidation states at the oxygen atoms (e.g. ozonides AO_3 (A = Na – Cs)[1,2] or sesquioxides A_2O_3 (A = K – Cs)[3]) as well as oxometalates with transition metals in their highest possible oxidation states (e.g. $Ag[MnO_4]$[4] or $Hg_4O_3[ReO_4]_2$[5] for members of group VII). The latter show barite-type crystal structures for the $A[MnO_4]$ cases with A = K – Cs,[6] whereas $Na[MnO_4]$[7] crystallizes isotypically with $Ag[MnO_4]$.[4] Only few examples of permanganates are known with a mixed counter-cation decoration (e.g. $Cs_3Ag[MnO_4]_4$[8]) so far. However, examples for analogous perrhenate compounds consisting of rhenium purely in its highest possible oxidation state +7 are less uncommon. They occur in various compounds either as tetrahedrally shaped *meta*-perrhenate anions $[ReO_4]^-$ (e.g. $RENa[ReO_4]_4$ (RE = Nd,[9,10] La, Sm – Gd[9])), as square pyramids $[ReO_5]^{3-}$ in *meso*-perrhenates such as $Sr_5[ReO_5]_3X$ (X = Cl, Br, I[11]) or as $[ReO_6]^{5-}$ octahedra in *ortho*-perrhenates (e.g. $A_5[ReO_6]$ with A = Li, Na[12]). Moreover, $[ReO_6]^{n-}$ octahedra with rhenium in various valence states are present within perovskite-type structures with the general composition $A_x[ReO_3]$ ($0 \le x \le 1$, such as $Sr_{0.4}ReO_3$;[13] note that x = 0 means ReO_3 itself[14]), $A_2B[ReO_6]$ (e.g. $Sr_2[(Cr,Re)O_6]$,[15] $Ba_2Mn[ReO_6]$[16]) or $AE_2A[ReO_6]$ (AE = Sr, Ba, A = Li, Na[17]), which are investigated due to their physical properties.

With all these pieces of information in mind, one might think of powerful redox-catalysts on the basis of the Mars-van-Krevelen mechanism, when the potential changes of the coordination numbers of the involved Re^{n+} (n = 5 – 7) cations could be overcome. We now report here on the serendipitously formed *meta*-perrhenate $CaNa[ReO_4]_3$, since no other element than rhenium with the atomic number 75 suits better for a dedicated publication on the occasion of a 75th anniversary of birth.

Results and Discussion

Crystal Structure

$CaNa[ReO_4]_3$ crystallizes isotypically to $ThCd[MoO_4]_3$[18] in the hexagonal space group $P6_3/m$ with the lattice parameters a = 991.74(6), c = 636.53(4) pm and c/a = 0.642 for Z = 2 (Table 1). Its crystal structure contains crystallographically unique Ca^{2+} cations surrounded by nine oxygen atoms forming a tricapped trigonal prism (d(Ca–O) = 6 × 249 pm + 3 × 254 pm) and unique Na^+ cations surrounded octahedrally by six oxygen atoms (d(Na–O) = 6 × 241 pm) (Figure 1). All of them belong to nearly ideal $[ReO_4]^-$ tetrahedra (d(Re–O) = 171 – 173 pm and ∡(O–Re–O) = 109–111°) formed by crystallographically unique Re^{7+} cations in the center, which are surrounded by four O^{2-} anions belonging to three different sites (Figure 1, Table 2 and Table 3). The triangular faces formed by the $(O3)^{2-}$ anions work as corners of the trigonal prisms of the $[CaO_9]^{16-}$ polyhedra, which are connected via three different perrhenate units with each other forming strands

* Prof. Dr. Th. Schleid
Fax: +49-711-6856-4241
E-Mail: schleid@iac.uni-stuttgart.de
[a] Institut für Anorganische Chemie
Universität Stuttgart
Pfaffenwaldring 55
70569 Stuttgart, Germany

along the [001] direction (Figure 2). The arrangement of these strands leads to the formation of large channels along the crystallographic *c*-axis, which are filled with Na^+ cations leading to chains of *trans*-face-shared $[NaO_6]^{11-}$ octahedra (Figure 3). Unlike the partially occupied Na^+ site in compounds such as $La_{0.75}Na_{0.75}[ReO_4]_3$[9] or $Nd_{0.75}Na_{0.75}[ReO_4]_3$[10] the Na^+ site in $CaNa[ReO_4]_3$ is fully occupied for reasons of charge compensation.

Table 1. Crystallographic data for $CaNa[ReO_4]_3$.

	$CaNa[ReO_4]_3$
Crystal system	hexagonal
Space group	$P6_3/m$ (no. 176)
a /pm	991.74(6)
c /pm	636.53(4)
c/a	0.642
Number of formula units, Z	2
Molar volume, V_m /cm³·mol^{-1}	163.26(4)
Calculated density, D_x /g·cm^{-3}	4.984(1)
Crystal color	colorless, transparent
Crystal shape	rod-shaped
Crystal size, V /mm³	0.044 × 0.023 × 0.018
Ranges, $2\theta_{max}$ /°; h, k, l	0.8 – 55.0; ±12, ±12, ±8
Diffractometer	κ-CCD (Bruker-Nonius)
Radiation	Mo-K_α (λ = 71.07 pm)
Monochromator	graphite
Temperature, T /K	293(2)
Absorption coefficient, μ /mm^{-1}	33.97
Transmission, min. / max.	0.204 / 0.628
Measured reflections	8756
Unique reflections	452
Observed reflections with $F_o \geq 4\sigma(F_o)$	427
R_{int} / R_σ	0.051 / 0.016
R_1 [a] / wR_2 [b] / GooF [c] (all reflections)	0.022 / 0.044 / 1.190
Residual electron density / 10⁶·pm^{-3} (max. /min.)	1.19 / –0.85

a) $R_1 = \Sigma \, ||F_o| - |F_c|| \, / \, \Sigma \, |F_o|$. b) $wR_2 = [\Sigma w(F_o^2 - F_c^2)^2 \, / \, \Sigma(wF_o^2)^2]^{1/2}$; $w = 1/[\sigma^2(F_o^2)+(xP)^2+yP]$ with $P = [(F_o^2)+2F_c^2]/3$. c) GooF: $S = [\Sigma w(F_o^2 - F_c^2)^2 \, / \, (n-p)]^{1/2}$, with n being the number of reflections and p being the number of parameters.

The Madelung Part of the Lattice Energy (MAPLE)[19–21] shows a perfect agreement between the value for $CaNa[ReO_4]_3$ (104210 kJ·mol^{-1}) and the sum of the respective binary oxides (CaO: 4035 v, Na_2O: 2907 kJ·mol^{-1}, Re_2O_7: 65798 kJ·mol^{-1}) according to MAPLE(CaO) + $^1/_2$ MAPLE(Na_2O) + $^3/_2$ MAPLE(Re_2O_7) = 4035 + 1453 + 98697 = 104185 kJ·mol^{-1}. This comes a little surprising, when one keeps in mind that octahedrally coordinated Ca^{2+} cations in NaCl-type CaO ($d(Ca^{2+}–O^{2-})$ = 240.6 pm, 6×),[22] tetrahedrally coordinated Na^+ cations in *anti*-CaF_2-type Na_2O ($d(Na^+–O^{2-})$ = 240.8 pm, 4×)[23] and four- and sixfold coordinated Re^{7+} cations in orthorhombic Re_2O_7 ($d(Re^{7+}–O^{2-})$ = 168–181 pm for C.N. = 4 and 165–216 pm for C.N. = 6)[24] are compared with ninefold coordinated Ca^{2+} cations ($d(Ca^{2+}–O^{2-})$ = 6 × 248.5 pm + 3 × 253.8 pm), sixfold coordinated Na^+ cations ($d(Na^+–O^{2-})$ = 6 × 241.4 pm) and just tetrahedrally coordinated Re^{7+} cations ($d(Re^{7+}–O^{2-})$ = 171–173 pm, C.N. = 4) in hexagonal $CaNa[ReO_4]_3$.

As already stated by *Rudolf Hoppe* in his pioneer articles on the MAPLE concept,[19,20] the actual nature of bonding is less important than expected, if one reduces the energy strictly to its electrostatic part. Considering trigonal low-quartz ($[SiO_{4/2}]$)[25] with vertex-connected $[SiO_4]^{4-}$ tetrahedra as more covalent than rutile-type stishovite ($[SiO_{6/3}]$)[26] suggesting a higher ionic portion within its edge- and vertex-sharing $[SiO_6]^{8-}$ octahedra, their very similar MAPLE values (15272 kJ·mol^{-1} for low-quartz vs. 15037 kJ·mol^{-1} for stishovite) appear very baffling. The same holds, whenever two binary oxides combine to a ternary one, as the example of perovskite-type $BaCeO_3$[27] with twelvefold coordinated Ba^{2+} cations and vertex-connected $[CeO_6]^{8-}$ octahedra as compared to halite-type BaO ($[BaO_{6/6}]$)[28] with octahedrally coordinated Ba^{2+} cations and fluorite-type CeO_2 ($CeO_{8/4}$)[29] with Ce^{4+} cations in cubic oxygen coordination shows. Although one cannot speculate about the driving force of this acid-base reaction, there is a coordinative winner (Ba^{2+} with C.N. = 12 coming from C.N. = 6) with higher bond ionicity and a coordinative loser (Ce^{4+} with C.N. = 6 coming from C.N. = 8) with higher bond covalency, if one neglects the fate of the transferred base (O^{2-}). On the basis of MAPLE calculations with MAPLE(BaO) = 3506 kJ·mol^{-1}, MAPLE(CeO_2) = 11948 kJ·mol^{-1} and MAPLE($BaCeO_3$) = 15472 kJ·mol^{-1}, the formation of $BaCeO_3$ from BaO and CeO_2 (MAPLE sum of the binaries: 15454 kJ·mol^{-1}) is energetically almost neutral. From this point of view, the formation of $CaNa[ReO_4]_3$ from CaO, Na_2O and Re_2O_7 has two coordinative winners (Ca^{2+} with C.N. = 9 coming from C.N. = 6 and Na^+ with C.N. = 6 coming from C.N. = 4) with higher bond ionicity, but only one loser (half of the Re^{7+} with C.N. = 4 coming from C.N. = 6, while the other half even remains at C.N. = 4) with higher bond covalency.

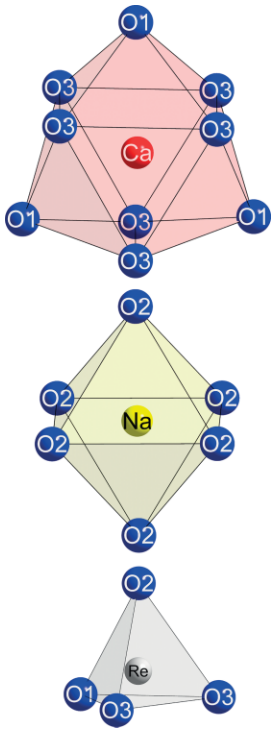

Figure 1. Tricapped trigonal prism $[CaO_9]^{16-}$ (top), octahedron $[NaO_6]^{11-}$ (mid), and tetrahedron $[ReO_4]^-$ (bottom) in the hexagonal crystal structure of $CaNa[ReO_4]_3$.

Table 2. *Wyckoff* sites, symmetry, fractional atomic coordinates, anisotropic and equivalent isotropic displacement parameters (U_{ij} /pm^2 [a)] and U_{eq} /pm^2 [b)]) for $CaNa[ReO_4]_3$.

Atom	Site	Symmetry	*x*/*a*	*y*/*b*	*z*/*c*	U_{11}	U_{22}	U_{33}	U_{23}	U_{13}	U_{12}	U_{eq}
Na	2*b*	$\bar{3}$..	0	0	0	292(18)	= U_{11}	24(3)	0	0	= $^1/_2U_{11}$	275(12)
Ca	2*c*	$\bar{6}$..	$^1/_3$	$^2/_3$	$^1/_4$	103(7)	= U_{11}	66(10)	0	0	= $^1/_2U_{11}$	90(5)
Re	6*h*	*m*..	0.39194(4)	0.29157(4)	$^1/_4$	162(2)	179(2)	172(2)	0	0	80(1)	173(2)
O1	6*h*	*m*..	0.4432(7)	0.4840(7)	$^1/_4$	273(31)	253(31)	301(32)	0	0	157(27)	264(13)
O2	6*h*	*m*..	0.1921(7)	0.1724(7)	$^1/_4$	184(30)	282(33)	338(36)	0	0	46(26)	300(14)
O3	12*i*	1	0.4670(5)	0.2529(5)	0.0309(7)	402(26)	307(24)	342(26)	22(20)	143(21)	188(21)	346(11)

a) The anisotropic displacement factor takes the form: $U_{ij} = \exp[-2\pi^2(h^2a^{*2}U_{11} + k^2b^{*2}U_{22} + l^2c^{*2}U_{33} + 2klb^*c^*U_{23} + 2hla^*c^*U_{13} + 2hka^*b^*U_{12})]$. b) U_{eq} is defined as one third of the orthogonalized U_{ij} tensor, here: $U_{eq} = {}^1/_3[U_{33} + {}^4/_3(U_{11} + U_{22} - U_{12})]$.

Table 3. Relevant interatomic distances (*d* /pm) and angles (/°) in $CaNa[ReO_4]_3$ with estimated standard deviations in parentheses.

Distance		Distance	
Ca–O3 (6×)	248.5(5)	Re–O1 (1×)	171.2(6)
Ca–O1 (3×)	253.8(6)	Re–O3 (2×)	171.2(5)
Na–O2 (6×)	241.4(4)	Re–O2 (1×)	172.7(6)
Angle		**Angle**	
O1–Re–O2 (1×)	111.3(2)	O2–Re–O3 (2×)	109.0(2)
O1–Re–O3 (2×)	109.2(2)	O3–Re–O3 (1×)	109.1(3)

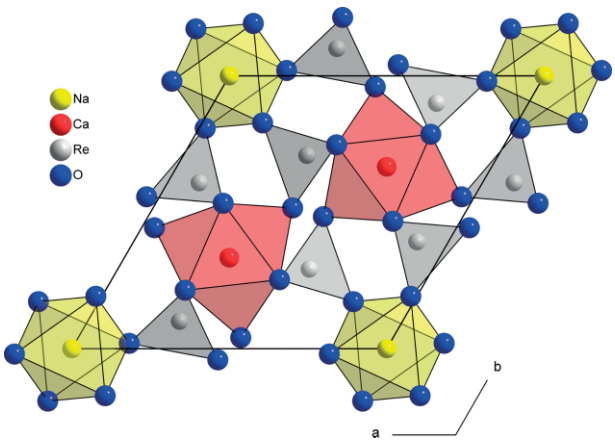

Figure 2. View along the [001] direction at the hexagonal unit cell of $CaNa[ReO_4]_3$.

The crystal structure of europium(III) perchlorate $Eu[ClO_4]_3$[30,31] represents a topotactically peroxidized example of the UCl_3-type structure of $EuCl_3$ (hexagonal, $P6_3/m$)[32] by transforming spherical Cl^- into tetrahedral $[ClO_4]^-$ anions and the ytterbium(III) perrhenate $Yb[ReO_4]_3$[33] crystallizes isotypically. Like sodium derivatives of UCl_3[34] tend to form stuffed variants of the mother structure (e.g. NaU_2Cl_6 written as U_2NaCl_6[35]), the lanthanoid(III) perrhenates do likewise (e.g. $Nd_{0.75}Na_{0.75}[ReO_4]_3$) with vacancies and mixed cationic distribution over the available six- and ninefold coordinated positions (according to $(Nd_{0.71}Na_{0.29})(Na_{0.56}\square_{0.44})[ReO_4]_3$[10]). With $CaNa[ReO_4]_3$ we now have the first example of a perrhenate in hands, which exhibits a perfect cationic order with Ca^{2+} in ninefold and Na^+ in sixfold coordination of oxygen atoms belonging to $[ReO_4]^-$ tetrahedra. This ordered arrangement is already known as $ThCd[MoO_4]_3$-type structure[18] among the oxidomolybdates(VI), but with Th^{4+} in ninefold and Cd^{2+} in sixfold oxygen coordination.

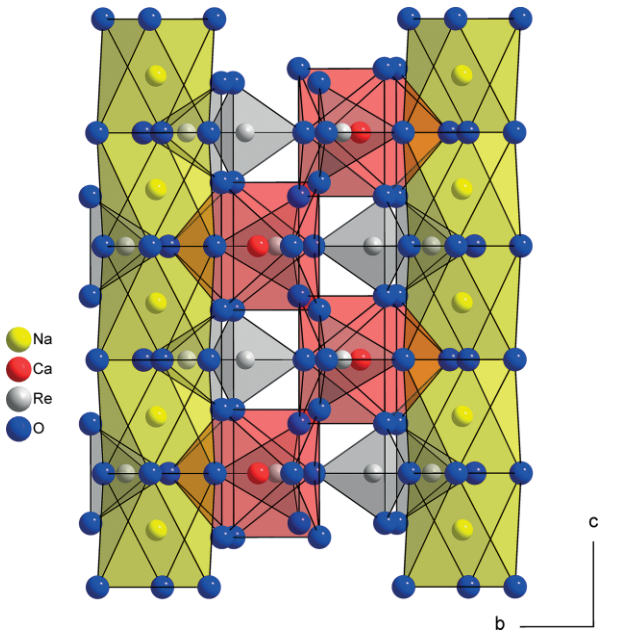

Figure 3. View along the [100] direction at the Na^+-filled channels along [001] and at strands of tricapped trigonal prisms $[CaO_9]^{16-}$ linked via three $[ReO_4]^-$ anions each.

PXRD Measurements

To confirm the success of the targeted synthesis of the title compound a Powder X-ray Diffraction (PXRD) pattern of the pestled sample was recorded (Figure 4), since the view through a polarization microscope at the $CaNa[ReO_4]_3$ sample showed no single crystals suitable for X-ray diffraction experiments.

The comparison of the observed pattern with a simulated one from the single-crystal data of $CaNa[ReO_4]_3$ revealed only a few reflections marked with asterisks not matching well (Figure 4). They can all be assigned to a small amount of $Ca[ReO_4]_2{\cdot}2H_2O$.[36]

EDXS Measurements

Energy Dispersive X-ray Spectroscopy (EDXS) was performed on the previously investigated single crystal of $CaNa[ReO_4]_3$ to determine the elements present within the sample. This was necessary, as the refinement of the single-crystal X-ray diffraction data did not yield a chemically rea-

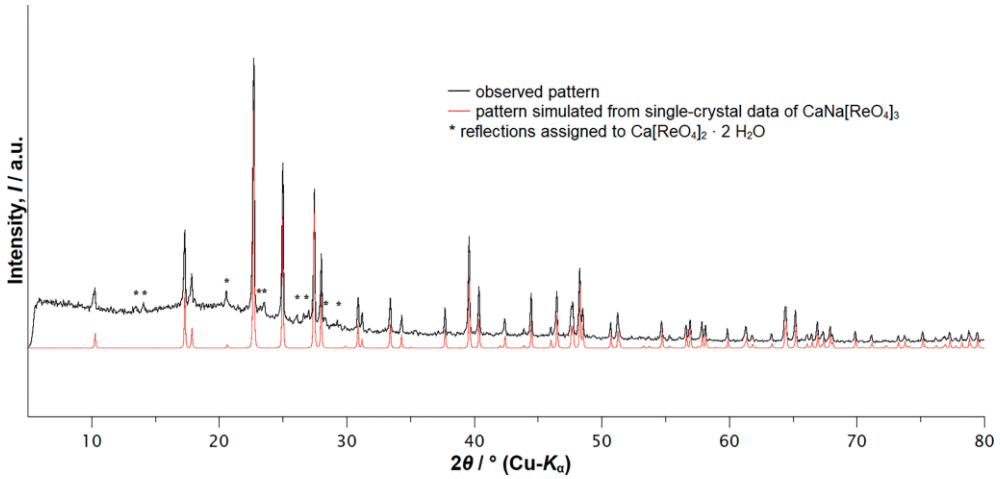

Figure 4. PXRD pattern of $CaNa[ReO_4]_3$ containing minor impurities of $Ca[ReO_4]_2{\cdot}2\,H_2O$ (black) compared to the pattern of $CaNa[ReO_4]_3$ simulated from single-crystal data (red). Reflections belonging to the side phase $Ca[ReO_4]_2{\cdot}2H_2O$[36] are marked with asterisks (*).

sonable structure model, if cerium is the only metal cation apart from rhenium contained within this compound. Moreover, the absence of barium and sulfur needed to be proven, since both were part of the initial salt-metathesis brine ($Ce[SO_4]_2$ and $Ba[ReO_4]_2$). The results of the qualitative EDXS measurement show that apart from oxygen, calcium, sodium and rhenium are the only ingredients of the sample as the O-K_α, Na-K_α, Ca-K_α and Re-M_α lines are clearly visible within the spectrum (Figure 5, top). Even though quantitative statements derived from a qualitative measurement should be made with great care, the measurement clearly shows that there are only marginal amounts of cerium either in the sample or more likely on its surface as the Ce-M_α and Ce-L_α lines are barely visible at all (Figure 5, top). The microcrystalline sample arising from subsequent targeted synthesis of $CaNa[ReO_4]_3$ was also investigated via EDXS also confirming the presence of exclusively calcium, sodium and rhenium aside from oxygen within the sample (Figure 5, bottom).

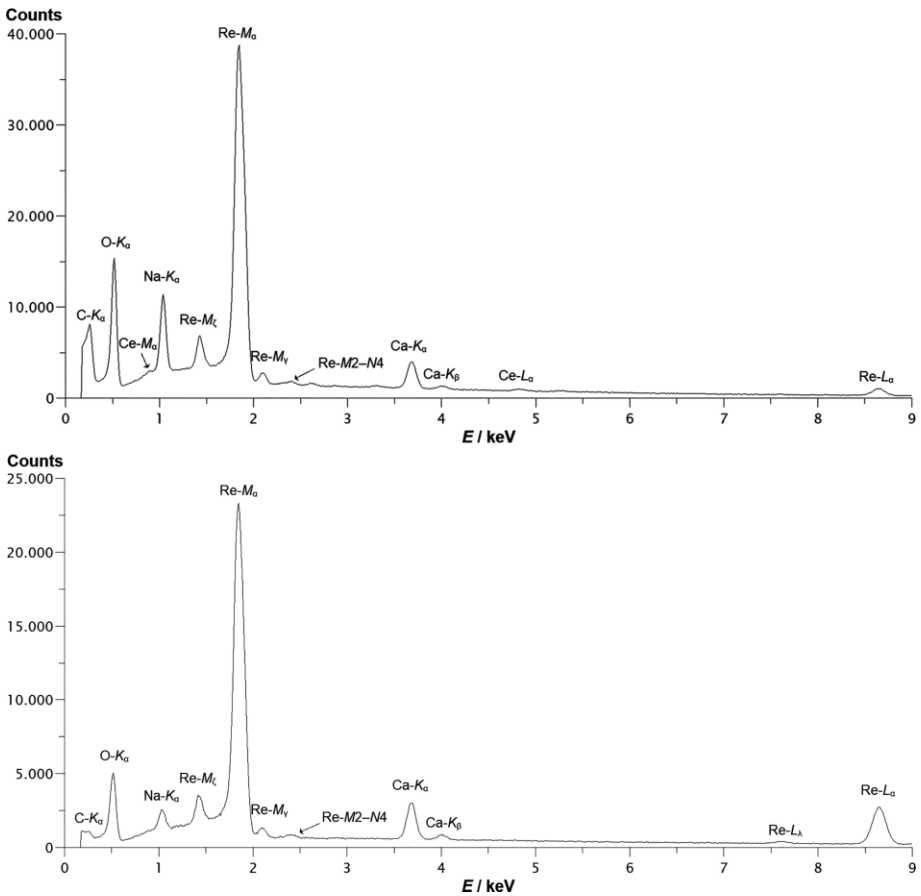

Figure 5. EDXS measurement for a single crystal of $CaNa[ReO_4]_3$ (top) and for microcrystalline $CaNa[ReO_4]_3$ (bottom).

Raman Spectroscopy

A comparison of the obtained Raman frequencies (Figure 6) for $CaNa[ReO_4]_3$ with data for the anhydrous ternary components $Na[ReO_4]$ and $Ca[ReO_4]_2$[37] shows that the quaternary phase displays almost all vibrations of both ternary ones (Table 4). This was expected as isolated $[ReO_4]^-$ anions are the linkers between both sorts of cations (Ca^{2+} and Na^+) within the $CaNa[ReO_4]_3$ structure, although scheelite-type $Na[ReO_4]$[38] displays eightfold coordinated Na^+ cations, whereas the coordination number of Ca^{2+} in anhydrous $Ca[ReO_4]_2$ has yet to be determined.

STA Measurements

Equimolar amounts of $Na[ReO_4]$ and $Ca[ReO_4]_2{\cdot}2\,H_2O$ crystallized from aqueous solution (see Exp. Sect.) were investigated by Simultaneous Thermal Analysis (STA) (Figure 7) to track the reaction of both components yielding polycrystalline $CaNa[ReO_4]_3$.

Table 4. Raman data of $CaNa[ReO_4]_3$ compared to the Raman frequencies (in cm^{-1}) reported for $Na[ReO_4]$ and $Ca[ReO_4]_2$ [a].

Mode	$Na[ReO_4]$ [37]	$Ca[ReO_4]_2$ [37]	$CaNa[ReO_4]_3$
ν(lattice)	77 (s)		57 (vw)
	84 (m)		76 (vw)
	129 (vw)		83 (vw)
			143 (vw)
$\delta([ReO_4]^-)$	324 (vw)	314 (vw)	309 (vw)
	333 (w)	338 (m)	315 (vw)
	371 (w)	344 (m)	334 (m)
		352 (m)	344 (s)
		367 (vw)	360 (s)
			369 (vw)
$\nu_{as}([ReO_4]^-)$	886 (m)	906 (m)	886 (w)
	924 (w)	914 (m)	896 (m)
		940 (m)	910 (m)
		969 (vw)	922 (vw)
			936 (w)
$\nu_s([ReO_4]^-)$	956 (vs)	991 (m)	956 (s)
		1006 (s)	979 (m)
			992 (vs)

a) (vw) very weak, (w) weak, (m) medium, (s) strong, (vs) very strong.

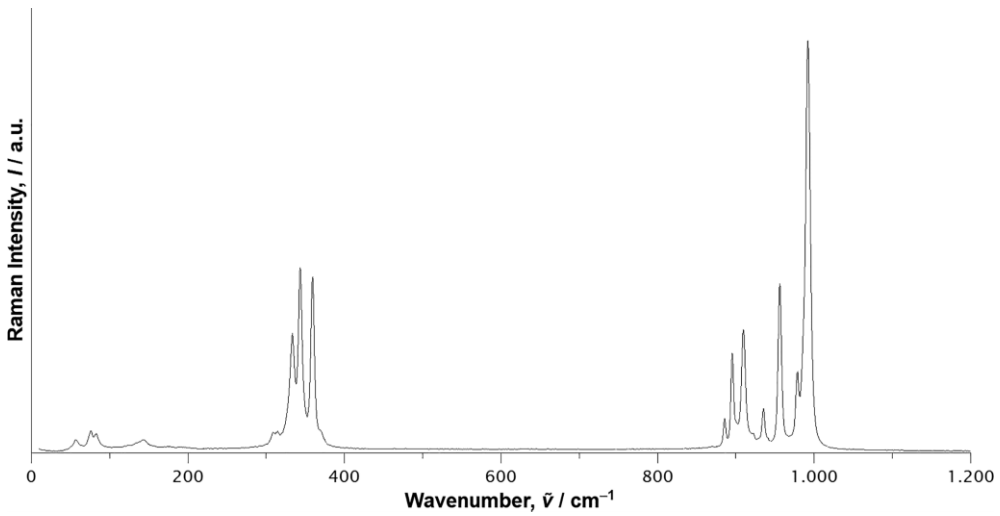

Figure 6. Raman spectrum of microcrystalline $CaNa[ReO_4]_3$.

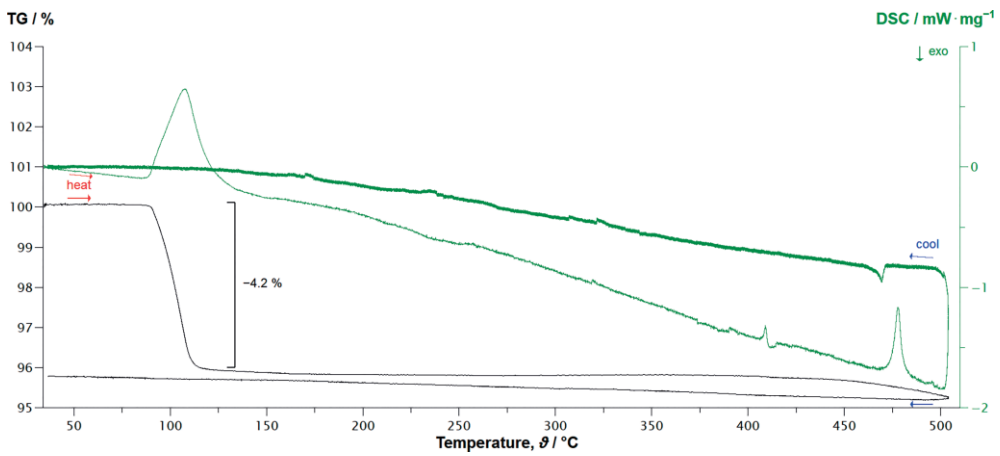

Figure 7. STA measurement of a mixture of $Na[ReO_4]$ and $Ca[ReO_4]_2{\cdot}2\,H_2O$ in a molar ratio of 1:1. The TG signal is shown in black and the DSC signal in green.

Heating the reaction mixture under inert gas conditions first leads to an endothermic signal at around 100 °C related to a mass loss of about 4 %, which is caused by evaporation of both water molecules of hydration from $Ca[ReO_4]_2{\cdot}2H_2O$. Upon further heating a small endothermic signal at 409 °C with no correlated mass loss is observed, which occurs at a slightly lower temperature than the literature known melting point of $Na[ReO_4]$ of 414 °C[39] most likely due to the formation of an eutectic mixture with $Ca[ReO_4]_2$. The last endothermic signal of the heating curve recorded at 478 °C and also not correlated with a change of mass belongs to the formation of $CaNa[ReO_4]_3$. When the reaction mixture, now a melt of $CaNa[ReO_4]_3$, is cooled back down an exothermic signal at 469 °C indicates the recrystallization process. Afterwards, there is neither a change of mass nor an energy signal visible during the cooling of the target product down to room temperature.

Conclusions

With $CaNa[ReO_4]_3$ we accidentally found single crystals of the first perrhenate with a mixed counter-cation combination in the $ThCd[MoO_4]_3$ type structure. The targeted and almost phase-pure synthesis of microcrystalline $CaNa[ReO_4]_3$ was possible by cooling down a melt of the anhydrous perrhenates $Na[ReO_4]$ and $Ca[ReO_4]_2$, whereas crystallization from aqueous solution only leads to the formation of the ternary border phases $Na[ReO_4]$ and $Ca[ReO_4]_2{\cdot}2H_2O$, which can be used advantageously as precursors for a successful solid-state reaction.

Experimental Section

Synthesis: All steps of the synthesis were performed under atmospheric conditions. First, barium perrhenate hydrate $Ba[ReO_4]_2{\cdot}H_2O$ was synthesized via cation exchange analogously to literature procedure[40] using potassium perrhenate $K[ReO_4]$ (99 %, Alpha Aesar, Karlsruhe, Deutschland) as precursor material and Amberlite IR-120 (Fluka AG, Buchs, Switzerland) as resin. After the cation exchange and subsequent isothermal evaporation drying the residual solution in a desiccator over silica gel for two days yielded colorless, transparent crystals of barium perrhenate monohydrate $Ba[ReO_4]_2{\cdot}H_2O$.

A compound containing tetravalent cerium and perrhenate anions such as $Ce[ReO_4]_4{\cdot}xH_2O$ was attempted to synthesize metathetically utilizing the low solubility of $Ba[SO_4]$ as driving force of the reaction. Thus to an aqueous solution of 16.2 mg (0.04 mmol) yellow $Ce[SO_4]_2{\cdot}4H_2O$ (pure, Merck, Darmstadt, Germany) a solution of 26.3 mg (0.04 mmol) white $Ba[ReO_4]_2{\cdot}H_2O$ in deionized water was added resulting in a total of 20 mL aqueous solution. Two hours of stirring and subsequently filtering off the emerging precipitation of white $Ba[SO_4]$ resulted in a pale yellow and clear solution, which was later transferred to a watch glass. After two days of isothermal evaporation at ambient conditions few colorless, transparent, rod-shaped single crystals of what turned out to be $CaNa[ReO_4]_3$ remained next to a black and X-ray amorphous side product.

In order to specifically synthesize $CaNa[ReO_4]_3$ on target, firstly perrhenic acid was generated via cation exchange analogously to literature procedure[41] using 194 mg (0.68 mmol) of potassium perrhenate $K[ReO_4]$ (99 %, Alpha Aesar, Karlsruhe, Germany) as precursor material and Amberlite IR-120 (Fluka AG, Buchs, Switzerland) as resin. Secondly, the resulting solution of perrhenic acid was added in excess to a moistened mixture of 17.2 mg (0.205 mmol) sodium hydrogen carbonate $Na[HCO_3]$ (99.5 %, Grüssing, Filsum, Germany) and 20.5 mg (0.205 mmol) calcium carbonate $Ca[CO_3]$ (p.a., Merck, Darmstadt, Germany) and subsequently evaporated under reduced pressure until approximately 5 mL of the colorless solution remained. Afterwards, this solution was transferred to a watch glass and dried overnight in a desiccator over silica gel yielding a mixture of sodium perrhenate $Na[ReO_4]$ and calcium perrhenate dihydrate $Ca[ReO_4]_2{\cdot}2H_2O$. Finally, 93 mg of the pestled mixture were filled into an open corundum crucible, dried overnight at 200 °C and subsequently heated to 500 °C in a muffle furnace with a heating rate of 10 $K{\cdot}min^{-1}$. Cooling the reaction mixture down to room temperature after roughly 5 minutes with a rate of 1 $K{\cdot}min^{-1}$ lead to the formation of colorless, microcrystalline $CaNa[ReO_4]_3$.

Crystallographic Studies: A polarization microscope was used to select a suitable single crystal of the title compound, which was subsequently sealed into a thin-walled glass capillary for the single-crystal X-ray diffraction experiments. Afterwards, the capillary was mounted on a Nonius κ-CCD diffractometer equipped with a Mo-K_α radiation source (λ = 71.07 pm), a graphite monochromator and a CCD detector. The collected intensity data were processed with the program DENZO[42] and a numerical absorption correction was applied using the HABITUS program.[43] After analysis of the systematic absences, only three possible space groups remained to be considered: $P6_3$ (no. 173), $P6_3/m$ (no. 176) and $P6_322$ (no. 182). At first no chemically reasonable solution could be found in any of the aforementioned space groups, but as EDXS analysis proved high calcium and sodium contents within the sample and barely any cerium a reasonable structure solution and refinement could be achieved in the space group $P6_3/m$. The crystal structure was solved by direct methods and subsequently refined using the SHELX-97 program package.[44–47] A list of the crystallographic data is shown in Table 1, the *Wyckoff* sites, the fractional atomic coordinates, the anisotropic and the equivalent isotropic displacement parameters can be found in Table 2, and relevant interatomic distances and angles of $CaNa[ReO_4]_3$ are listed in Table 3.

Further details of the crystal structure investigations may be obtained from the Fachinformationszentrum Karlsruhe, 76344 Eggenstein-Leopoldshafen, Germany (Fax: +49-7247-808-666; E-Mail: crysdata@fiz-karlsruhe.de, http://www.fiz-karlsruhe.de/request for deposited data.html) on quoting the depository number CSD-1897786 for the title compound.

PXRD Measurements: The collection of the powder X-ray diffraction pattern took place at room temperature in atmospheric conditions on a labscale powder diffractometer in Debye-Scherrer setup (STOE, Darmstadt, Germany) equipped with a Cu-K_α radiation source (λ = 154.18 pm), a curved Johannson-type germanium (111) monochromator and an image plate position sensitive detector. About 5 mg of the previously pestled sample were placed on top of an adhesive tape fixed at an aluminum inlet fixated in a sample carrier, which was rotated during the measurement. The pattern was measured in the range of 2θ = 5 – 80° applying a total scan time of 20 min. The theoretical pattern of the single-crystal data was simulated using the program $WinX^{POW}$.[48]

EDXS Measurements: After the single-crystal X-ray diffraction measurement the very single crystal of $CaNa[ReO_4]_3$ was transferred from the thin-walled glass capillary onto a conductive carbon pad (Plano G3347) and subsequently vaporized with carbon in order to avoid charging effects on the surface. The experiments were conducted on a Cameca SX-100 (Paris, France) electron microprobe equipped with

an energy-dispersive spectrometer. Three separate measurements were carried out at different locations of the crystal surface with an acceleration voltage of 15 kV, a beam current of 15 nA with an irradiation time of 60 s. Measurements and data collection were made using NSS 3.1 (Thermo Scientific, Madison, WI, USA). Afterwards, for the EDXS measurements of the second synthesis attempt a small amount of the coarse-grained pounded powder was prepared analogously. However, in this case the acceleration voltage was 20 kV with a beam current of 10 nA and an irradiation time of 60s. The experiment was repeated at three different locations on various crystallites.

Raman Spectroscopy: A powder comprising of mostly $CaNa[ReO_4]_3$ and small amounts of $Ca[ReO_4]_2{\cdot}2\,H_2O$ was filled in a thin-walled glass capillary and Raman spectroscopic measurements were conducted using an XploRA microscope LASER Raman Spectrometer (Horbia Jobin Yvon, Bensheim, Germany, 25 mW, equipped with a green LASER with an excitation line at λ = 532 nm, 50 × magnification, 15 × 2 s accumulation time). With no ν(O–H) vibration observed at 3200–3600 cm^{-1}, it can be stated that the Raman spectrum of the selected crystallite was not corresponding to the water-containing side product $Ca[ReO_4]_2{\cdot}2\,H_2O$, but to the main phase consisting of $CaNa[ReO_4]_3$.

STA Measurements: For the simultaneous thermal analysis a STA 449 C Jupiter device (NETZSCH, Selb, Germany) was used. After conducting a buoyancy correction 14.33 mg (0.018 mmol) of equimolar amounts of thoroughly pestled and mixed $Na[ReO_4]$ and $Ca[ReO_4]_2{\cdot}2\,H_2O$ were given into a corundum crucible covered by a lid with a small hole in it. The sample was heated to 500 K with a rate of 5 K/min and subsequently cooled back down to room temperature with 1 $K{\cdot}min^{-1}$ in a constant argon gas flow.

Acknowledgements

The authors are grateful for the financial support of the Federal State of Baden-Württemberg. Furthermore, we thank *Dr. Falk Lissner* for the single-crystal XRD, *Felix C. Goerigk* (M.Sc.) for the EDXS measurements, *Kevin U. Bareiß* (M.Sc.) for the Raman and *Patrik Djendjur* (M.Sc.) for the STA measurements. Open access funding enabled and organized by Projekt DEAL.

Keywords: Crystal structure; MAPLE; Raman spectroscopy; Calcium sodium perrhenate; Single-crystal X-ray diffraction

References

[1] W. Schnick, M. Jansen, *Angew. Chem. Int. Ed. Engl.* **1985**, *24*, 54–55.
[2] M. Jansen, H. Nuss, *Z. Anorg. Allg. Chem.* **2007**, *633*, 1307–1315.
[3] A. Sans, J. Nuss, G. H. Fecher, C. Mühle, C. Felser, M. Jansen, *Z. Anorg. Allg. Chem.* **2014**, *640*, 1239–1246.
[4] F. M. Chang, M. Jansen, *Z. Kristallogr.* **1984**, *169*, 295–298.
[5] B. E. Prasad, J. Nuss, C. Felser, M. Jansen, *Z. Anorg. Allg. Chem.* **2016**, *642*, 1359–1363.
[6] R. Hoppe, D. Fischer, J. Schneider, *Z. Anorg. Allg. Chem.* **1999**, *625*, 1135–1142.
[7] J. M. Bauchert, H. Henning, Th. Schleid, *Z. Naturforsch. B* **2016**, *71*, 993–995.
[8] J. M. Bauchert, H. Henning, Th. Schleid, *Z. Anorg. Allg. Chem.* **2012**, *638*, 1780–1783.
[9] Z. A. A. Slimane, J. P. F. Silvestre, W. Freundlich, *Compt. Rend. Seanc. Acad. Sci. C* **1978**, *287*, 409–410.
[10] S. Grupe, M. S. Wickleder, *Z. Anorg. Allg. Chem.* **2003**, *629*, 955–958.
[11] M. S. Schriewer, W. Jeitschko, *J. Solid State Chem.* **1993**, *107*, 1–11.
[12] T. Betz, R. Hoppe, *Z. Anorg. Allg. Chem.* **1984**, *512*, 19–33.
[13] G. Baud, J. P. Besse, R. Chevalier, B. L. Chamberland, *J. Solid State Chem.* **1979**, *28*, 157–162.
[14] K. Meisel, *Z. Anorg. Allg. Chem.* **1932**, *207*, 121–128.
[15] M. T. D. Orlando, A. S. Cavichini, J. B. Depianti, J. L. Passamai, J. R. Rocha, J. F. Salvador, C. G. P. Orlando, *J. Alloys Compd.* **2016**, *687*, 463–469.
[16] J. M. Longo, R. Ward, *J. Am. Chem. Soc.* **1961**, *83*, 2816–2818.
[17] M. Bharanthy, H. C. zur Loye, *J. Solid State Chem.* **2008**, *181*, 2789–2795.
[18] S. Launay, A. Rimsky, *Acta Crystallogr., Sect. B* **1980**, *36*, 910–912.
[19] R. Hoppe, *Angew. Chem. Int. Ed. Engl.* **1966**, *5*, 95–106.
[20] R. Hoppe, *Angew. Chem. Int. Ed. Engl.* **1970**, *9*, 25–34.
[21] R. Hübenthal, MAPLE; Program for the Calculation of the Madelung Part of Lattice Energy, University of Gießen, Germany **1993**.
[22] I. Oftedal, *Z. Phys. Chem.* **1927**, *128*, 154–158.
[23] E. Zintl, A. Harder, B. Dauth, *Z. Elektrochem. Angew. Phys. Chem.* **1934**, *40*, 588–593.
[24] B. Krebs, A. Müller, H. H. Beyer, *Inorg. Chem.* **1969**, *28*, 436–443.
[25] H. d'Amour, W. Denner, H. Schulz, *Acta Crystallogr., Sect. B* **1979**, *35*, 550–555.
[26] W. Sinclair, A. E. Ringwood, *Nature* **1978**, *272*, 714–715.
[27] S. K. Knight, *Solid State Ionics* **1994**, *74*, 109–117.
[28] R. J. Zollweg, *Phys. Rev.* **1955**, *100*, 671–673.
[29] J. D. McCullough, *J. Am. Chem. Soc.* **1950**, *72*, 1386–1390.
[30] J. L. Pascal, F. Favier, F. Cunin, A. Fitch, G. Vaughan, *J. Solid State Chem.* **1998**, *139*, 259–265.
[31] M. S. Wickleder, *Z. Anorg. Allg. Chem.* **1999**, *625*, 11–12.
[32] B. Morosin, *J. Chem. Phys.* **1968**, *49*, 3007–3012.
[33] V. N. Khrustalev, M. B. Varfolomeev, N. B. Shamrai, Yu. T. Struchkov, A. P. Pisarevskii, *Koord. Khim.* **1993**, *19*, 871–872.
[34] Th. Schleid, G. Meyer, L. R. Morss, *J. Less-Common Met.* **1987**, *132*, 69–77.
[35] Th. Schleid, G. Meyer, *Naturwissenschaften* **1989**, *76*, 118–118.
[36] W. H. Baur, D. Kassner, *J. Solid State Chem.* **1992**, *100*, 166–169.
[37] K. Ulbricht, H. Kriegsmann, *Z. Anorg. Allg. Chem.* **1968**, *358*, 193–209.
[38] J. Beintema, *Strukturbericht* **1937**, *3*, 421–423.
[39] W. T. Smith Jr., S. H. Long, *J. Am. Chem. Soc.* **1948**, *70*, 354–356.
[40] H. Henning, J. M. Bauchert, M. Conrad, Th. Schleid, *Z. Naturforsch. B* **2017**, *72*, 555–562.
[41] K. Leszczyńka-Sejda, G. Benke, A. Chmielarz, S. Krompiec, S. Michalik, *Hydrometallurgy* **2007**, *89*, 289–296.
[42] Z. Otwinowski, W. Minor, *Methods Enzymol.* **1997**, *276*, 307–326.
[43] W. Bärnighausen, H. Herrendorf, HABITUS, Program for the Optimization of the Crystal Shape for Numerical Absorption Correction in X-SHAPE, Karlsruhe, Gießen (Germany), **1993**.
[44] G. M. Sheldrick, *SHELXS-97*: Program for the Solution of Crystal Structures, Univ. Göttingen, Germany **1997**.
[45] G. M. Sheldrick, *Acta Crystallogr., Sect. A* **1990**, *46*, 467–473.
[46] G. M. Sheldrick, *SHELXS-97*: Program for the Refinement of Crystal Structures, Univ. Göttingen, Germany **1997**.
[47] G. M. Sheldrick, *Acta Crystallogr., Sect. A* **2008**, *64*, 112–122.
[48] STOE & Cie GmbH, $WinX^{POW}$ Version 3.0.1.13, Software Package for Powder Diffraction, Darmstadt, Germany **2009**.

Received: August 9, 2019
Published Online: November 13, 2019

